Polymer 51 (2010) 6037–6046

Contents lists available at ScienceDirect

Polymer

journal homepage: www.elsevier.com/locate/polymer

Different thermal behaviors of microbial polyesters poly(3-hydroxybutyrate-*co*-3-hydroxyvalerate-*co*-3-hydroxyhexanoate) and poly(3-hydroxybutyrate-*co*-3-hydroxyhexanoate)

Hai-Mu Ye [a,1], Zhen Wang [b,1], Hong-Hui Wang [b], Guo-Qiang Chen [c,**], Jun Xu [a,*]

[a] *Dept Chemical Engineering, Key Laboratory of Advanced Materials of Ministry of Education, Tsinghua University, Beijing 100084, PR China*
[b] *Multidisciplinary Research Center, Shantou University, Shantou 515063, PR China*
[c] *Dept Biology, School of Life Science, Tsinghua University, Beijing 100084, PR China*

ARTICLE INFO

Article history:
Received 8 February 2010
Received in revised form
22 September 2010
Accepted 13 October 2010
Available online 20 October 2010

Keywords:
Poly(3-hydroxybutyrate-*co*-3-hydroxyhexanoate)
Poly(3-hydroxybutyrate-*co*-3-hydroxyvalerate-*co*-3-hydroxyhexanoate)
Multiple melting behavior

ABSTRACT

Various methods were employed to study the thermal behaviors of a novel microbial polyhydroxyalkanoate (PHA) terpolyester, namely, poly(3-hydroxybutyrate-*co*-3-hydroxyvalerate-*co*-3-hydroxyhexanoate) (PHBVHHx) compared with poly(3-hydroxybutyrate-*co*-3-hydroxyhexanoate) (PHBHHx). PHBVHHx showed higher crystallization rate and degree of crystallinity. PHBVHHx exhibited also different multiple melting behaviors from PHBHHx. The WAXD results demonstrated that the crystal lattice of PHBVHHx was more compact than that of PHBHHx, suggesting stronger interaction between chain stems. DSC and *in-situ* heating WAXD studies revealed that PHBVHHx showed a partial melting-lamellar thickening-remelting process during heating, while PHBHHx demonstrated a melting-rapid formation of new crystals-remelting process. It is proposed that the simultaneous introduction of 3-hydroxyvalerate and 3-hydroxyhexanoate monomers into poly(3-hydroxybutyrate) improves the mobility of chain stems along the chain direction, leading to easier intralamellar slip during heating or drawing, further resulting in improvement of mechanical properties, which was supported by the DMA tests. Consequently, we establish a relationship between the thermal behavior and the mechanical properties of biodegradable plastics, which we believe is applicable to other polymers as well.

1. Introduction

Polyhydroxyalkanoates (PHA) are microbial polyesters produced by many microorganisms. They have attracted much attention for their biodegradability, biocompatibility and the comparable mechanical properties with commercial non biodegradable plastics [1–3]. Poly(3-hydroxybutyrate) (PHB) is the first member of PHA family; which shows high melting point (~c.a. 180 °C) and tensile strength, but brittleness and low elongation at break ($\varepsilon_b < 5\%$) at room temperature due to its higher degree of crystallinity limits its applications. Comonomers, such as 3-hydroxyvalerate (3HV) and 3-hydroxyhexanoate (3HHx), have been introduced into PHB, resulting in formation of PHBV and PHBHHx, which display a broad range of thermal and mechanical properties varying with comonomer content. For instance, the elongation at break (ε_b) and decomposition temperature of PHBV and PHBHHx increase with increasing comonomer content in a certain range, widening their processing window and application areas. However, aging is a serious problem for the semi-crystalline PHA. PHB, PHBV and PHBHHx age rather quickly over time even at room temperature, exhibiting reduction of ε_b due to increase of brittleness [4–7]. Furthermore, the introduction of 3HV or 3HHx monomers results in significant reduction on the crystallization rate and on the degree of crystallinity, which is disadvantageous for their processing including injection molding, film blowing and fiber spinning. Recently, a microbial terpolyester PHBVHHx containing 3HB, 3HV and 3HHx monomers was synthesized by recombinant *Aeromonas hydrophila* 4AK4 harboring *phbA* and *phbB* (*phaAB*) genes encoding β-ketothiolase and acetoacetyl-CoA reductase of *Ralstonia eutropha* [8,9]. It was reported that simultaneous incorporation of 3HV and 3HHx improved the ductility and rigidity of the polyester compared with PHBV and PHBHHx with similar comonomer contents. Mechanical properties of these PHAs from literatures are listed in Table 1. For example, the cast film of poly (3HB-*co*-5.4 mol% 3HV-*co*-11.7 mol% 3HHx) terpolyester showed a rather high elongation at break up to 340%, and the tensile strength was still maintained at about 15.7 MPa. In contrast, PHBHHx12 film

* Corresponding author. Tel.: +86 10 62784740; fax: +86 10 62784550.
** Corresponding author. Tel.: +86 10 62783844; fax: +86 10 62794217.
E-mail addresses: chengq@mail.tsinghua.edu.cn (G.-Q. Chen), jun-xu@mail.tsinghua.edu.cn (J. Xu).
[1] Both authors contributed equally to this study.

0032-3861/$ – see front matter © 2010 Elsevier Ltd. All rights reserved.
doi:10.1016/j.polymer.2010.10.030

Table 1
The mechanical properties of PHBHHx and PHBVHHx from literatures.

PHA (mol%)			Young's modulus (MPa)	Elongation at break (%)	Tensile strength (MPa)
HB	HV	HHx			
[a]88	0	12	134.8	107.7	4.5
[a]82.9	5.4	11.7	290.5	340.1	15.7
[b]72.8	16.8	10.4	97.0	739.7	14.3

[a] The mechanical properties are adopted from ref. [8].
[b] The mechanical properties are adopted from ref. [9].

demonstrated a low elongation at break around 108% and the tensile strength is only 4.5 Mpa [8]. The excellent mechanical properties of PHBVHHx terpolyester will greatly widen the application range of PHAs.

As is well known, the physical and mechanical properties of semi-crystalline polymers are quite related to their crystal structures and thermal history. Various methods have been applied to characterize the crystallization and melting properties of different PHA homopolymers and copolymers containing two types of monomers [10–25]. However, crystallization and melting behaviors of PHAs consisting of three types of monomers of 3HB, 3HV and 3HHx are not yet studied.

In this paper, thermal behaviors of PHBVHHx terpolyesters are compared with that of PHBHHx in order to understand why terpolyester PHBVHHx exhibits improved mechanical properties over PHBHHx.

2. Experimental materials

2.1. Microbial production of PHA terpolyesters

Poly(3HB-*co*-12 mol% 3HHx) (PHBHHx12) was produced by *A. hydrophila* 4AK4 in MS medium [26] supplemented with 8 g/L of lauric acid. *R. eutropha* PHB-4 [27] harboring plasmid pZWJ4-31 [28] which contains PHA synthesis *phaPCJ* operon of *A. hydrophila* 4AK4 was used for biosynthesis of poly(3HB-*co*-3HV-*co*-3HHx) (PHBVHHx). The recombinant was cultured in MS medium supplemented with 5 g/L of octanoate and different concentrations of propionate as co-substrate. Poly(3HB-*co*-7 mol% 3HV-*co*-11 mol% 3HHx) (PHBV7HHx11) and poly(3HB-*co*-18 mol% 3HV-*co*-11 mol% 3HHx) (PHBV18HHx11) were obtained when 0.5 and 1.5 g/L of propionate were provided as precursor for HV monomer, respectively.

2.2. Characterization of physical properties

2.2.1. Extraction, purification and molecular weight study of PHA

The process of extraction and purification, and the following detection of monomer compositions and molecular weights were described by Wang et al. [29]. Table 2 shows the molecular weights of the three PHA samples.

2.2.2. Thermal and crystallization behavior studies

A Shimadzu DSC-60 apparatus was used to study the isothermal crystallization from the melt state and the following melting process. PHA samples were heated to a temperature about 30 °C higher than their melting points, holding for 2 min to completely eliminate the thermal history, and then quickly quenched to a predetermined temperature for a sufficient time to obtain the isothermally crystallized samples. After that, samples were heated directly from the isothermal temperature to melt at a heating rate of 10 °C/min. The DSC apparatus was calibrated with indium standard and nitrogen atmosphere was used throughout the study.

Table 2
Molecular weights and molecular weight distribution of PHBV7HHx11, PHBV18HHx11 and PHBHHx12.

Sample	M_w (g/mol)	M_n (g/mol)	M_w/M_n
PHBV7HHx11	1.60×10^6	7.90×10^5	2.03
PHBV18HHx11	1.84×10^6	8.51×10^5	2.16
PHBHHx12	3.46×10^5	2.84×10^5	1.22

Other heating rates were used when examining the effect of heating rate on the melting behavior.

The morphologies and radial growth rates of PHA samples isothermally crystallized at different temperatures were observed by a Nikon polarized optical microscope (POM) equipped with a Panasonic CCD camera. Each sample was melted at the temperature about 30 °C higher than its melting point for 2 min and then quickly transferred to a preset isothermal hot-stage for isothermal crystallization. The *in-situ* Fourier transform infrared spectroscopy (FTIR) experiments were carried out on a Nicolet-560 spectrometer with a manually controlled heater. The PHA films were cast on KBr salt window from 20 mg/mL chloroform solution. After removal of the solvent, the samples were melted for 2 min and then placed at 75 °C to allow sufficient crystallization. After that, the prepared samples were heated and the FTIR spectra were collected at interval of 10 °C. Each was calculated by averaging 32 scans at a resolution of 4 cm^{-1} from 4000 cm^{-1} to 400 cm^{-1}.

The wide angle X-ray diffraction (WAXD) analyses were performed at room temperature using a Rigaku D/max2550HB+/PC X-ray diffractometer with Cu Kα radiation. The samples were scanned from 10° to 40° with a step interval of 0.02° at a scan rate of 4°/min. And the *in-situ* WAXD observation of the heating process of PHA samples was carried out on a Bruker D8 ADVANCE equipment, the 2θ angle was ranged from 10° to 26°, with a step interval of 0.02° at a scan rate of 6°/min. Two-dimensional WAXD pattern of PHBHHx12 and PHBV7HHx11 fibers were obtained on a Rigaku R-Axis Spider instrument with a Mo target. The wavelength of the X-ray of Mo was 0.708 Å and the beam size was 300 μm in diameter.

The mechanical damping tanδ of the PHA films was recorded on a dynamic mechanical analyzer (DMA-2980, TA Instruments) from −50 °C to 150 °C at a frequency of 1 Hz and a heating rate of 3 °C/min. The PHA samples were isothermally crystallized at 90 °C and then cut into the dimension of 40 × 5 × 0.3 mm.

3. Results and discussion

3.1. Crystallization behavior

The crystallization rate and degree of crystallinity of PHBHHx12 are lower than those of PHB due to the incorporation of non-crystallizable 3HHx comonomers, which limits the application of PHBHHx. Whereas, when 3HV and 3HHx comonomers are simultaneously introduced, the material becomes more ductile [8]. The improved properties may result from the higher crystallinity of PHBVHHx than that of PHBHHx. Table 3 shows the melting enthalpy (ΔH_m) and the radial growth rate of the spherulite of the three PHA samples. Both PHBVHHx samples exhibit higher ΔH_m

Table 3
Thermal parameters of the three PHA samples.

Sample	ΔH_m (90 °C) (J/g)	v (80 °C, POM) (μm/min)	v (90 °C, POM) (μm/min)	$t_{1/2}$ (90 °C, DSC) (min)
PHBV7HHx11	40.2	10.6	9.8	7.9
PHBV18HHx11	25.5	6.3	4.5	8.3
PHBHHx12	21.2	1.9	1.0	14.7

and growth rate than PHBHHx12 does even though they contain similar 3HHx contents. Especially, PHBV7HHx11 shows almost a twice ΔH_m value that of PHBHHx12, and much higher crystallization rate, almost 5 times at 80 °C and 10 times at 90 °C measured by POM. Furthermore, PHBV7HHx11 shows a growth rate two orders larger than PHBHHx with 17 mol% 3HHx (PHBHHx17), though both of them contain almost the same total comonomer content. The growth rate of PHBHHx17 reported by Xu et al. [30] was only around 1 nm/s at 75 °C. In addition, PHBV7HHx11 spherulite has a much larger band spacing than PHBHHx12, namely the lamellae of the former twist weaker than the latter (Fig. 1). Thus, the results show that the simultaneous introduction of 3HV and 3HHx monomers into PHB enhances the crystallization ability compared with PHBHHx copolymer.

The Avrami equation is usually used to describe the crystallization mechanism. Table 4 shows the Avrami exponent n of these three PHAs isothermally crystallized at different temperatures. The value of n is around 3 for PHBHHx12 at the studied T_cs, while around 2 for the two PHBVHHx samples. The different n values suggest different growth styles for the two types of PHAs, namely, three-dimensional growth of PHBHHx12 and two-dimensional growth of PHBVHHx (resulting from low nucleating density and thus large spherulite diameter), which accord with the result in Fig. 1. All the three samples crystallize via heterogeneous nucleation.

Since significant differences of the thermal properties existed between the PHBVHHx and PHBHHx12, more experiments were conducted to examine the melting behaviors during the heating processes (Fig. 2). DSC was utilized to study the melting process of PHBV7HHx11 and PHBHHx12 after their isothermal crystallization from melt at different crystallization temperatures (T_cs) for twice of the time needed to finish the apparent crystallization process. To prevent any possible changes during the cooling process, the samples were directly heated from T_c to melting. There are three endothermal peaks labeled as T_a, T_{m1} and T_{m2}, with the order $T_a < T_{m1} < T_{m2}$. Both T_a and T_{m1} peaks of PHBVHHx shift to a higher temperature with increasing T_c while the T_{m2} peak remains almost constant. Variance of the melting points with T_c is shown in Fig. 3a and b. The first melting peak T_a is approximately 8 °C higher than T_c and the fitting line of peak T_a is parallel to $T_m = T_c$ line. T_a observed here is called annealing peak, which may be due to melting of the imperfect crystallite or the transition of rigid amorphous fraction [20,31]. The annealing peak is not the focus of this study, thus in the following part we will concentrate on T_{m1} and T_{m2}. The melting peak T_{m1} increases linearly with T_c at the examined temperature range. The equilibrium melting point is 166 °C and 163 °C for the two terpolyesters extrapolated by linear Hoffmann–Weeks plot, while the highest melting peak T_{m2} remains almost constant around 143 °C and 141 °C for PHBV7HHx11 and PHBV18HHx11, respectively.

Table 4
The Avrami exponent n of the three PHA samples isothermally crystallized at different T_c.

Sample	T_c (°C)	n
PHBHHx12	75	2.88
	81	2.90
	92	3.09
	96	2.99
PHBV7HHx11	80	2.09
	86	2.12
	92	2.06
	96	2.03
PHBV18HHx11	80	2.24
	86	2.30
	92	2.06
	96	2.08

The T_c dependence of multiple melting peaks of PHBHHx12 is presented in Fig. 3c. The fitting curves of T_{m1} and T_{m2} are almost parallel to each other with a constant gap of around 20 °C, and they cross with the linear curve of $T_m = T_c$ at 146 °C and 167 °C, respectively. Hu et al. [20] attributed the appearance of T_{m2} in PHBHHx to the melting-recrystallization-remelting process by judging from the dependence of the multiple melting behavior on the heating rate. However, it is of interest to note that both T_{m1} and T_{m2} arise with T_c. As for most polymers, the remelting peak temperature is nearly independent of T_c. The abnormal phenomenon observed here will be discussed below.

The *in-situ* observation of PHA samples using POM is presented in Fig. 4 to visualize the heating process. The recrystallization occurred at around 135 °C for PHBV7HHx with the crystal brightness recovered at a certain extent. But the brightness of PHBHHx12 during heating process weakened continuously, which is due to its smaller fraction of recrystallization compared to the melted fraction. The real-time POM observation agrees with the DSC results shown in Fig. 2.

3.2. Effect of crystal form and chain conformation

The multiple melting peaks in poly(vinylidene fluoride) and polypropylene have been attributed to the coexistence of multiple crystal modifications [32,33]. To confirm whether the multiple melting peaks of PHB copolymers resulted from this reason, WAXD diffractograms of PHBV7HHx11, PHBV18HHx11 and PHBHHx12 were recorded at room temperature after being isothermally crystallized at 75 °C for sufficient time (Fig. 5). All samples exhibit the similar diffraction pattern as α-form PHB, though the positions of the diffraction peaks shift slightly. The α-form PHB possesses the orthorhombic cell parameters: a = 5.76 Å, b = 13.20 Å and

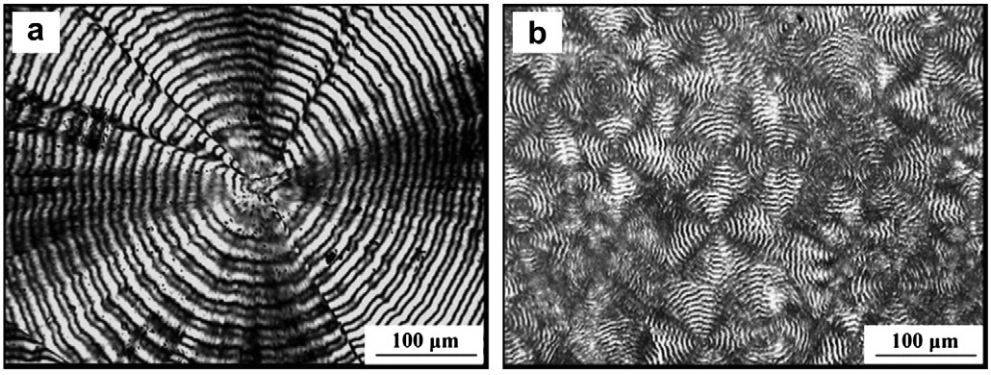

Fig. 1. The banded spherulite morphologies of (a) PHBV7HHx11 and (b) PHBHHx12 isothermally crystallized at 90 °C.

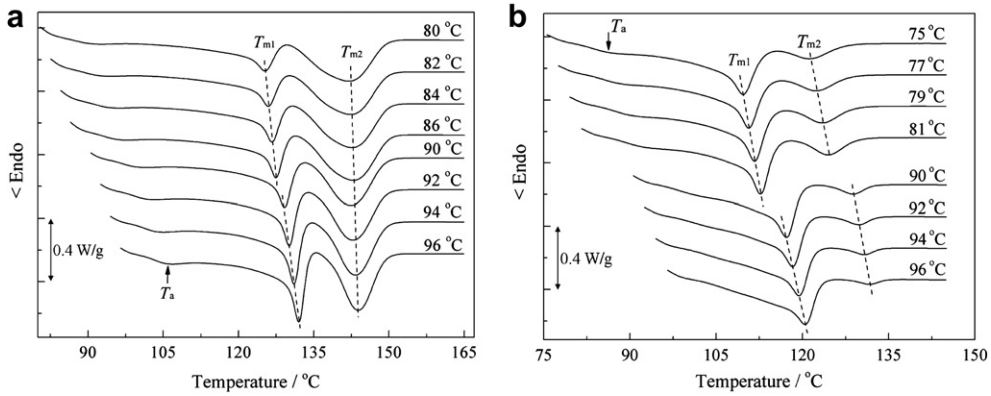

Fig. 2. The DSC curves of the melting process of (a) PHBV7HHx11 and (b) PHBHHx12 after being crystallized isothermally from melting state at different crystallization temperatures.

$c = 5.96$ Å [34,35]. We calculated from Fig. 5a–c to generate the unit cell parameters of PHA samples: $a = 5.76$ Å, $b = 13.24$ Å for PHBV7HHx11; $a = 5.78$ Å, $b = 13.26$ Å for PHBV18HHx11, and $a = 5.79$ Å, $b = 13.38$ Å for PHBHHx12, respectively. Furthermore, the two-dimensional WAXD results of PHBHHx12 and PHBV7HHx11 fibers are the same as shown in Fig. 5d and e, and the values of *c*-axis for PHBV7HHx11 and PHBHHx12 are 6.20 Å and 6.17 Å. So the packing densities are 1.209 and 1.196 g/cm^3 for PHBV7HHx11 and PHBHHx12, respectively. The characteristic diffraction of the β-form crystal is not observed [36,37]. Thus, the multiple melting peaks of PHAs studied here must be attributed to the same crystal modification. The *in-situ* WAXD observation on the melting behaviors of PHBHHx and PHBVHHx also confirmed the existence of a single crystal modification (Fig. 6 a and b). FTIR spectra of the three samples reveal no observable difference (Fig. 7), suggesting that the polymer chains adopt the same conformation. *In-situ* heating FTIR spectra recorded during the heating process of PHBV7HHx11 (Fig. 8) exhibit the same transition as those of PHBHHx12, which was also reported by Xu et al. [18] and Hu et al. [20]. The wave number of the carbonyl band shifts from 1724 cm^{-1} to 1740 cm^{-1} (Fig. 8b) and the bands corresponding to crystal structure, e.g., 1278 cm^{-1} and 1228 cm^{-1} (Fig. 8a), weaken during heating. The above WAXD and FTIR results confirm that PHBHHx and PHBVHHx adopt the same crystal modification and chain conformation. Consequently, the multiple melting behaviors of PHAs appear not to be a result of different crystal forms or chain conformations.

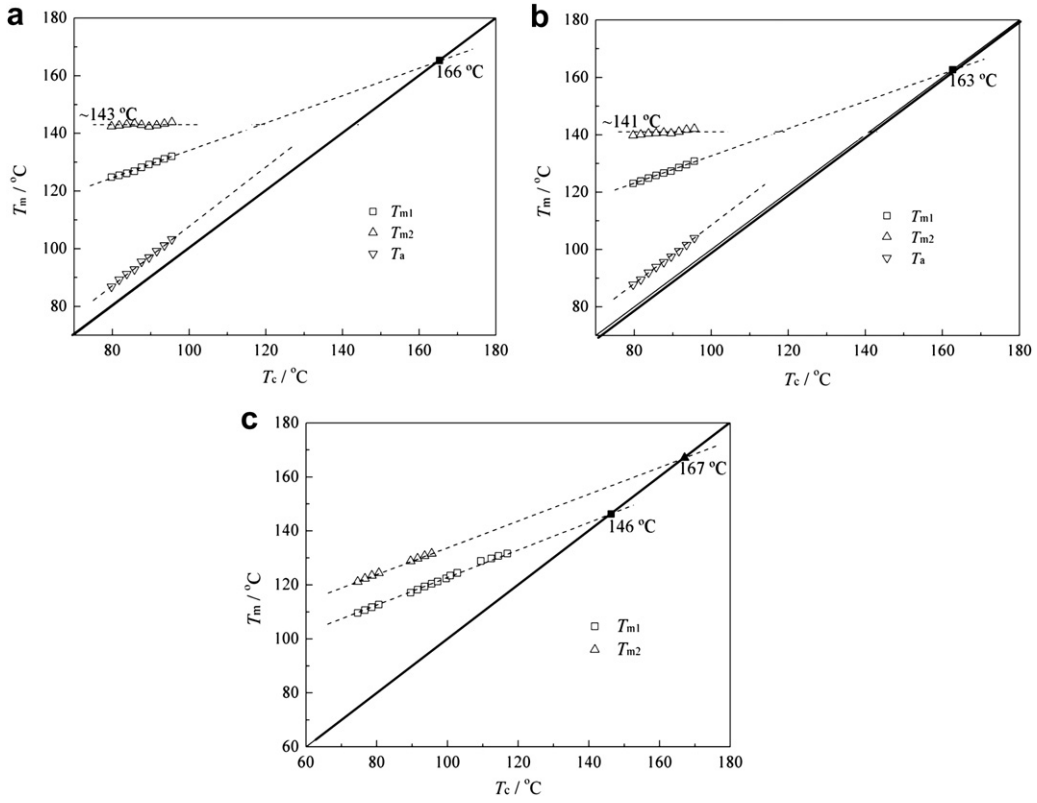

Fig. 3. The T_c dependence of the multiple melting points of (a) PHBV7HHx11, (b) PHBV18HHx11, and (c) PHBHHx12.

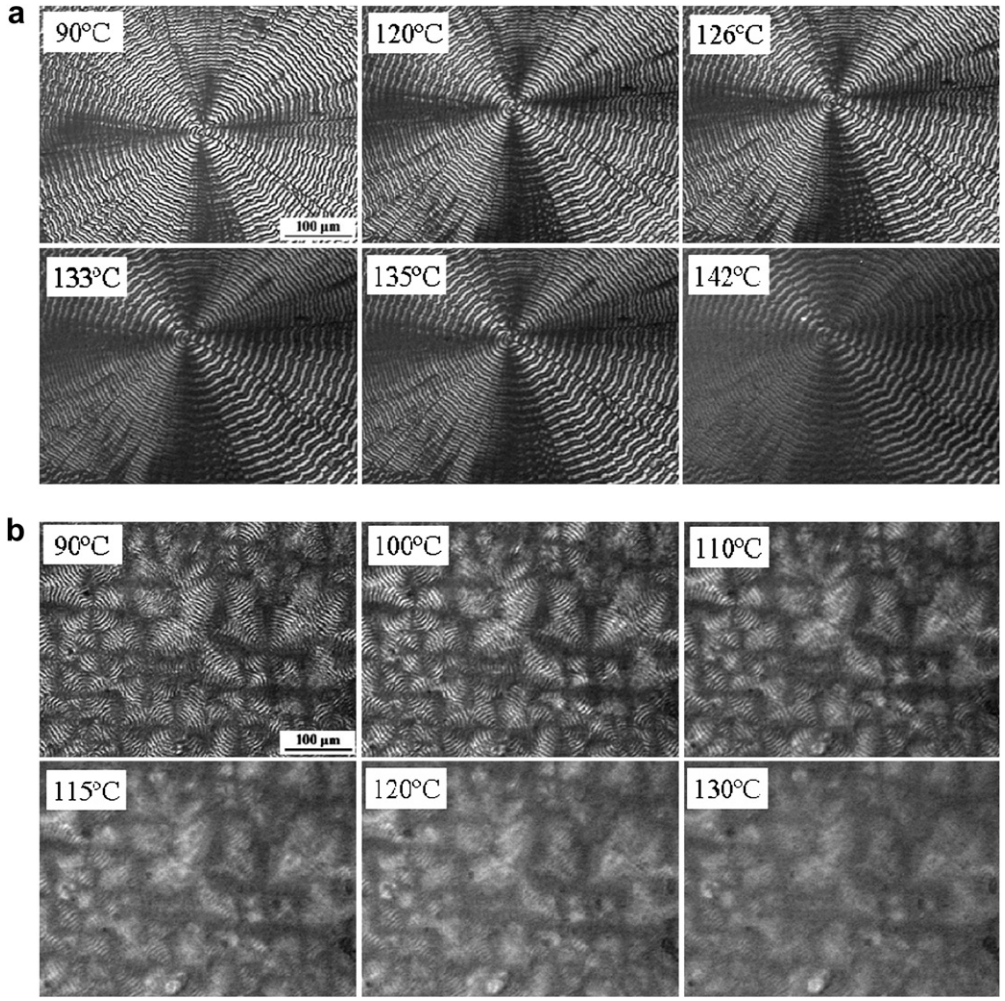

Fig. 4. The *in-situ* observation of (a) PHBV7HHx11 and (b) PHBHHx12 by POM at a heating rate of 10 °C/min after sufficiently crystallized at 90 °C.

3.3. The melting-recrystallization mechanism

Multiple melting peaks on DSC curve are usually observed in polyesters during the heating run, and most of the cases are attributed to the melting–recrystallization–remelting mechanism, yet the detail of the process was not much described. However, this mechanism can not answer the following questions: Why does T_{m2} peak of PHBHHx12 previously assigned as the melting peak of recrystallized part show almost the same tendency as the T_{m1} peak? And why does PHBVHHx display different melting behaviors from PHBHHx?

We suggest that the fitting line of T_{m2} of PHBHHx12 may just be a shift of the fitting line of T_{m1} (Fig. 3c). Above all, T_{m2} is due to the melting of recrystallized structure. If T_{m2} is just a shifting of T_{m1}, it should follow the same Hoffmann–Weeks plot. The start melting temperature (T_{sm1}) or the peak melting temperature T_{m1} is tentatively considered as the recrystallization temperature (T_{rc}). Surprisingly, when using $T_{rc} = T_{sm1}$, the T_{rc} dependence of T_{m2} plot falls perfectly on the fitting line of T_{m1}, as indicated by the half-filled square points in Fig. 9.

When T_{rc} was equal to T_{sm1} , the recrystallization process should occur very quickly (for it just happened around T_{sm1}). Thus, it is hypothesized that PHBHHx12 forms new crystals quickly just after it begins to melt at T_{sm1}. Fig. 10a shows the melting DSC curves of PHBHHx12, isothermally crystallized at 75 °C and held at T_{m1} (=110 °C) for different periods of time. The heating program is shown in Fig. 10d. The sample held at T_{m1} was in the partial melting state. It was expected that the longer the holding time, the more the recrystallized part and this should lead to a larger melting enthalpy of T_{m2}. However, the height of peak T_{m2} remained constant at 0.17 W/g, whatever the holding time was, with T_{sm1} equal to 97.3 °C. As shown in Fig. 10b, when the holding temperature was above T_{sm1}, the fusion of peak T_{m2} was independent of both the temperature and holding time. These indicate that the recrystallization would finish quickly as far as the temperature passed through T_{sm1}; otherwise, the melting enthalpy of peak T_{m2} should increase as the holding time prolonged. The melting enthalpy of peak T_{m2} in PHBHHx12 was much lower than that of PHBV7HHx11, while the melting enthalpy of peak T_{m1} in these two PHAs is similar (see Fig. 2), revealing that the recrystallization fraction is much less in PHBHHx12. The similar melting processes of PHBV7HHx11 are shown in Fig. 10. When held at T_{m1}, the peak height of T_{m2} increased with prolonging holding time, which is quite different from PHBHHx12.

To investigate the heating rate dependence of multiple melting behavior, we heated the samples at different rates to observe whether the ratio of the two peaks would change with heating rates. The decrease of the ratio of T_{m2} peak to T_{m1} peak was observed in PHBV7HHx11 (Fig. 11a), which is a common phenomenon of the melting-recrystallization mechanism. However, to our surprise, the

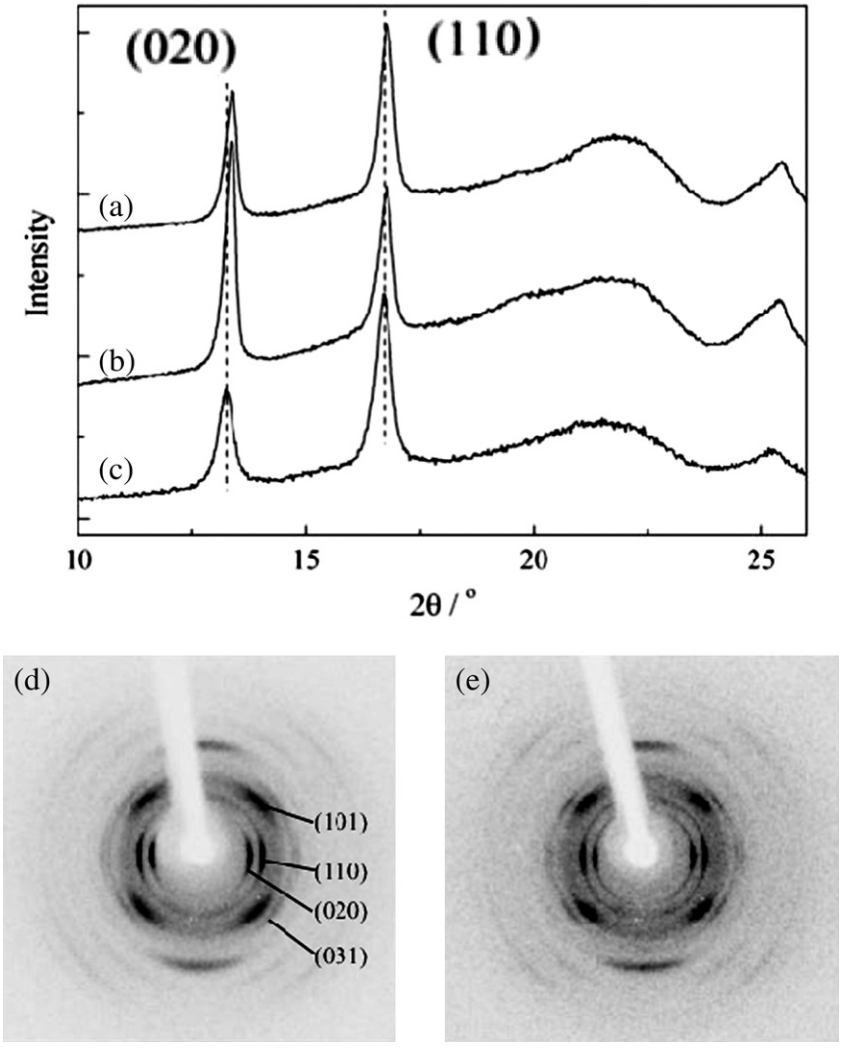

Fig. 5. The wide angle X-ray diffraction patterns of (a) PHBV18HHx11, (b) PHBV7HHx11, and (c) PHBHHx12. And the two-dimensional WAXD patterns of (d) PHBV7HHx11 fiber and (e) PHBHHx12 fiber.

T_{m2} peak was still prominent even at the heating rate of 40 °C/min, which might indicate that the reorganization synchronously proceeded with partial melting of original PHBV7HHx11 lamellae. In contrast, with the increase of heating rate from 5 °C/min to 40 °C/min, T_{m1} and T_{m2} of PHBHHx12 shifted simultaneously toward higher temperature, and the endothermal T_{m2} peak gradually diminished and disappeared eventually (Fig. 11b), suggesting that T_{m2} peak corresponds to the melting of the new crystals reformed during the heating process.

From the above results, it is speculated that the recrystallization of PHBV7HHx11 should be a reorganization process, e.g., via lamellar thickening, after partial melting of lamellae, which is difficult to eliminate by simply raising the heating rate. In addition, the thickening process requires the adjustment of chain stems in lamellae, making it more dependent on holding time. As a result, more original lamellae will transform into thicker lamellae. As lamellar thickening goes on, the energy barrier for intralamellar slip increases, and the kinetics finally leads to the thicker lamellae with almost a constant thickness, whatever T_c the original lamellae were formed. Thus, T_{m2}, the melting point of the thickened lamellae, is independent of T_c.

In-situ WAXD observation of the melting processes of PHA samples crystallized at 90 °C are shown in Fig. 6a and b. For PHBHHx12, the intensity of (020) and (110) diffraction planes decreased as the temperature increased until around 118 °C, and the intensity maintained almost constant from 118 °C to 126 °C, which should result from the recrystallization, then further increase of temperature led to further attenuation of diffraction peaks. During the whole process, the intensity ratio $I_{(110)}/I_{(020)}$ kept nearly a constant value about 1.5. The *in-situ* WAXD results of PHBHHx12 confirm the melting-recrystallization mechanism expected from DSC experiments. The constant diffraction intensity between 118 °C and 126 °C indicates that the total mass of crystal is constant under a certain heating rate as described in Fig. 10a. Unlike PHBHHx12, PHBV7HHx11 showed rather different change, the intensity of (020) plane decreased as the temperature rose to 132 °C, while the (110) plane first increased slightly and the ratio of $I_{(110)}/I_{(020)}$ increased from 0.7 to 1.0. The opposite change tendency of (020) plane and (110) plane should arise from the asynchronous reorganization of the two planes during the lamellar thickening process. It has been reported that the intensity ratio of (110) and (020) diffraction of PHB varies with the isothermal crystallization temperature [38]. The variation of the intensity ratio of (110) and (020) diffraction in PHBV7HHx11 during heating can be attributed to the different size or the different reorganization rates of (110) and (020) plane during the lamellar thickening process through

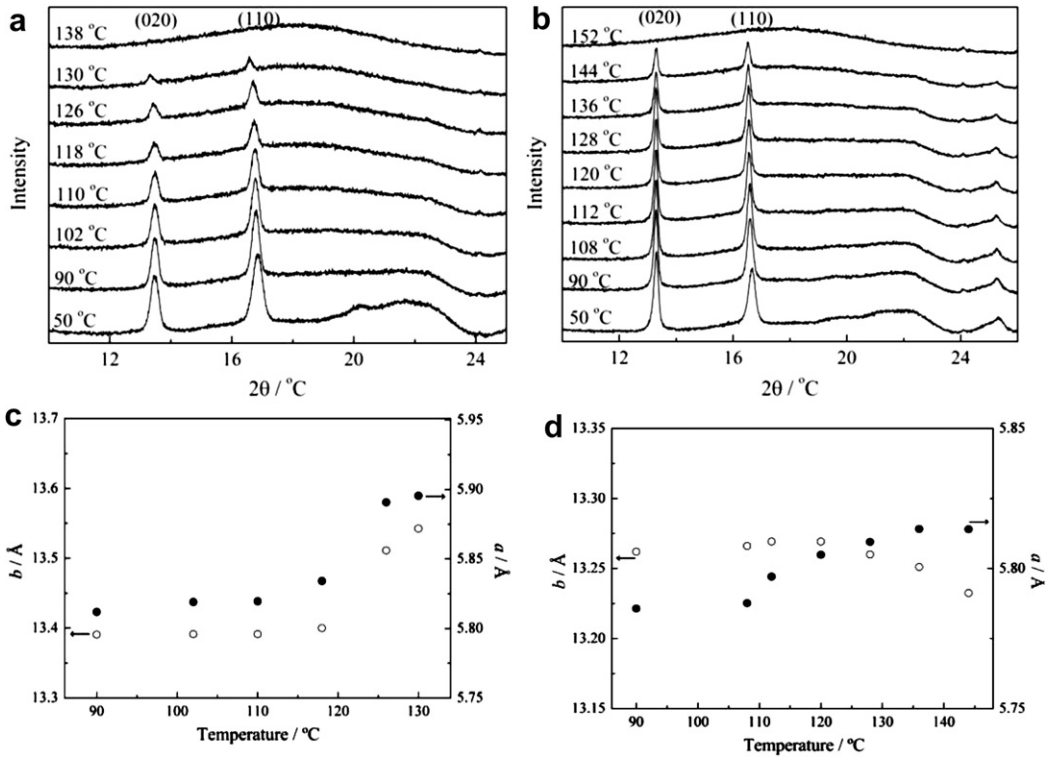

Fig. 6. The *in-situ* heating WAXD spectra of (a) PHBHHx12, and (b) PHB V7HHx11. Variation of the cell parameters of crystal lattice with temperature is presented in (c) for PHBHHx12 and (d) for PHBV7HHx11.

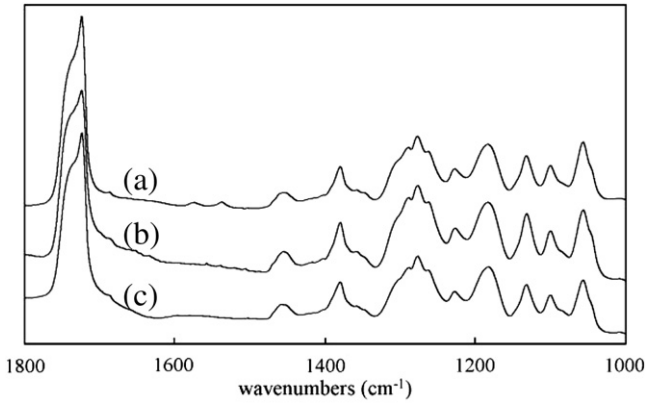

Fig. 7. The FTIR spectrograms of (a) PHBV7HHx11, (b) PHBV18HHx11 and (c) PHBHHx12.

intralamellar slip. Above 132 °C, further heating resulted in the synchronous decrease of both (020) and (110) planes, with the $I_{(110)}/I_{(020)}$ ratio remained constant at 1.0, which could also validate the above discussion. In the temperature range of T_{m2}, PHBV7HHx11 showed the similar behavior as PHBHHx12, which indicates the normal melting of newly formed thicker lamellae.

Fig. 6c and d present the heating influence on the values of *a* and *b* of the unit cell in the crystal lattice. In PHBHHx12, both *a* and *b* increase with the temperature during heating. In PHBV7HHx11, *a* value shows the same tendency as that in PHBHHx12, but increases more slowly, while *b* value first slightly increases and then slightly decreases (The relative variation of *b* is smaller than that of *a*). The different change of cell parameters further comfirms the different recrystallization process of PHBHHx12 and PHBV7HHx11.

Therefore, the different melting behaviors of PHBV7HHx11 and PHBHHx12 reflect the different mechanisms of recrystallization: the former corresponds to partial melting of lamellae–lamellar thickening–remelting mechanism while the latter corresponds to

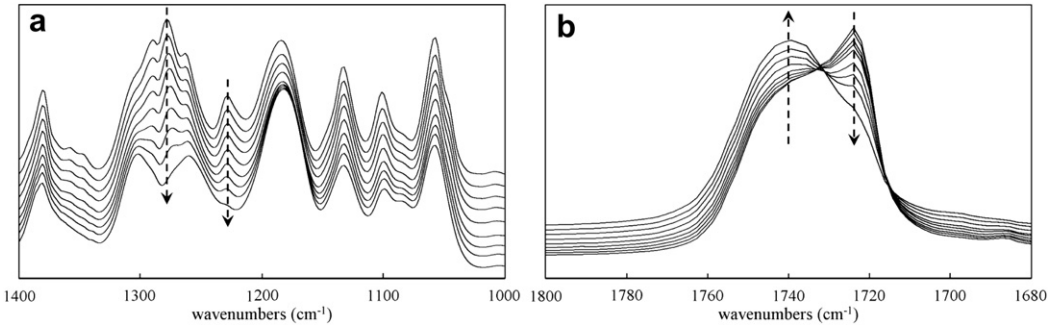

Fig. 8. The *in-situ* FTIR spectrograms of PHBV7HHx11 heated from 30 °C to 170 °C.

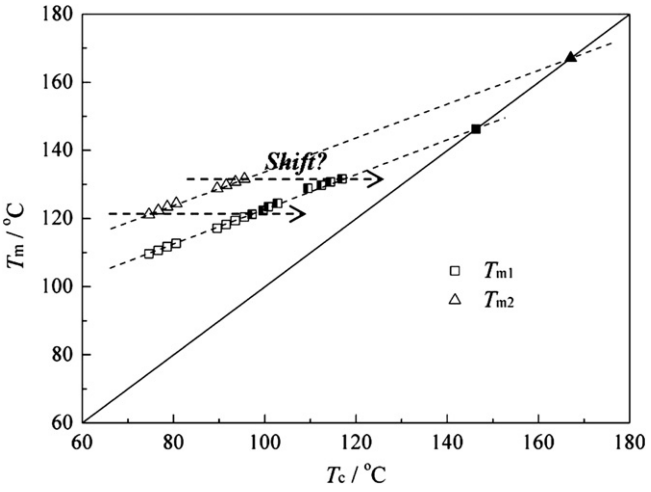

Fig. 9. The proposed shift from T_{m2} line to T_{m1} line in PHBHHx12.

melting-quickly formation of new lamellar crystals-remelting mechanism.

3.4. Why did PHBVHHx and PHBHHx follow different recrystallization manners?

Why did PHBVHHx and PHBHHx follow different recrystallization manners? We attributed it to different degree of interaction between neighboring chain stems in the lamellar crystals. The *a* and *b* values of PHBHHx12 are larger than those of PHBV7HHx11, which indicate that there is stronger interaction between the neighboring stems in PHBV7HHx11 than PHBHHx12. In PHB and its copolyesters, the hydrogen bonding between neighboring stems is along *a* axis [39]. The smaller *a* value, the stronger hydrogen bonding in PHA [40]. Consequently, the different parameters suggest that there is stronger hydrogen boding in the PHBVHHx terpolyesters than in PHBHHx.

It was reported that 3HHx monomers were excluded from the crystalline part and enriched mainly on the amorphous fold surfaces [41], while 3HV monomers coexisted both in crystalline and amorphous part [42], thus, the large distortion of the unit cell parameter of the crystalline lattice should be resulted from the overcrowding of non crystallizable comonomers on the lamellar surface. Because 3HV can co-crystallize with 3HB, while 3HHx are enriched on the lamellar surface, the 3HV monomers in the crystalline part might alleviate the surface stresses, which result in smaller lattice parameters and larger band spacing for PHBV7HHx11 and PHBV18HHx11 (Fig. 1a). The co-crystallization of HV with HB monomer units might be the reason for the higher crystallization rate and higher degree of crystallinity in PHBVHHx compared with PHBHHx12.

During the heating process, PHBHHx12 crystal structure was easily destroyed due to the weaker interaction between neighboring chain stems, as indicated by the larger crystal cell expansion than PHBV7HHx11 (see Fig. 6c). The lamellar crystals of PHBHHx12 were melted immediately from the start melting temperature. In the meanwhile, a small amount of polymer chains recrystallized into more stable lamellae in the presence of unmelted lamellar nuclei, with the T_{m2} peak just belonging to the more stable lamellae. Both PHBVHHx samples possessed stronger interaction

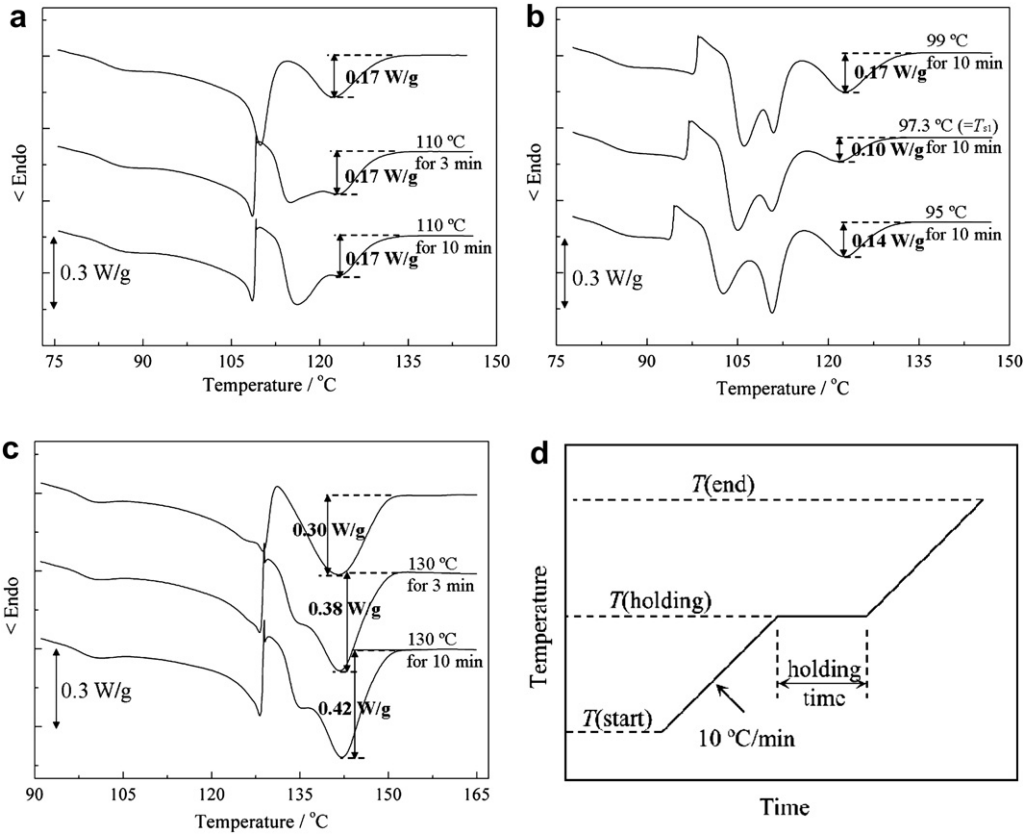

Fig. 10. The melting DSC curves of (a) PHBHHx12, isothermally crystallized at 75 °C, then kept at T_{m1} (=110 °C) for different holding time, (b) PHBHHx12, isothermally crystallized at 75 °C, then kept at different holding temperatures for 10 min, and (c) PHBV7HHx11, isothermally crystallized at 90 °C, then kept at T_{m1} (=130 °C) for different holding time, and (d) the sketch of heating program.

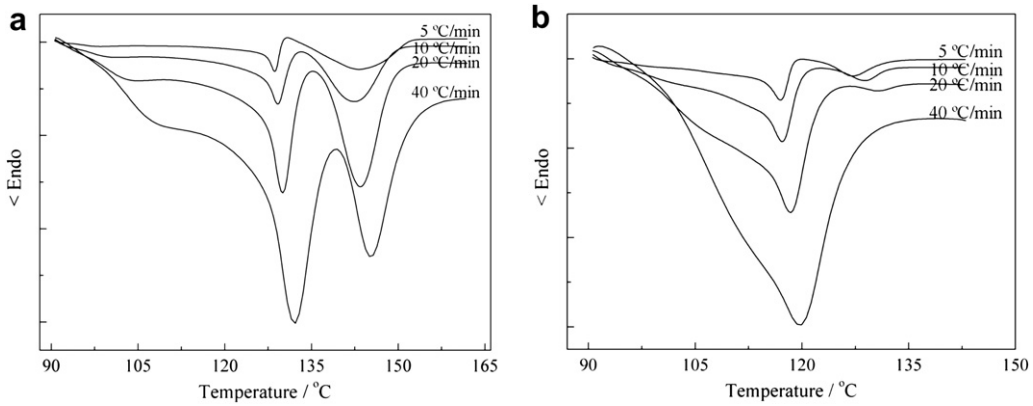

Fig. 11. The DSC curves of (a) PHBV7HHx11 and (b) PHBHHx12 in the heating run under different heating rates.

between neighboring chain stems than PHBHHx12 did, contributing to higher stability of the PHBVHHx lamellae. When heated, there is less crystal cell expansion in PHBVHHx (Fig. 6d). The lamellar thickening process in PHBVHHx happened due to chain sliding before the complete destruction of the crystal structure. Thus, the different interaction between neighboring stems led to the different melting behaviors of the three PHA samples.

At the similar 3HHx comonomers content, PHBVHHx showed higher tensile strength as a result of its higher degree of crystallinity and stronger hydrogen bonding than PHBHHx. Similar to heating, tensile drawing might also cause intralamellar slip and reorganization of lamellae in PHBVHHx, resulting in a high elongation at break. Fig. 12 shows the DMA testing results of the three PHA samples. During the whole testing temperature range, PHBVHHx samples exhibited lower damping tangent than PHBHHx12, resulting from the higher degree of crystallinity of the former. PHBHHx12 sample showed a sudden increase of tanδ when passed through T_{m1}, which can be attributed to the melting of most original lamellae with a small part of new lamellae formed from recrystallization at the same time. In contrast, PHBVHHx samples demonstrated slow and steady increase, which indicate that a large amount of lamellae underwent reorganization during the heating process, resulting in a slower melting process. The DMA results agree with the DSC results shown in Fig. 2, where PHBVHHx presents a much larger T_{m2} peak than PHBHHx. These results also reveal the easier tendency of lamellar reorganization in PHBVHHx. Our results demonstrate that there is a close link between the lamellar reorganization during heating and tensile drawing, which both result from the motion of chain stems in the lamellar crystals. Consequently, we may estimate the mechanical properties from the thermal behavior if there is only tiny sample size, where determination of the mechanical properties is a challenging issue.

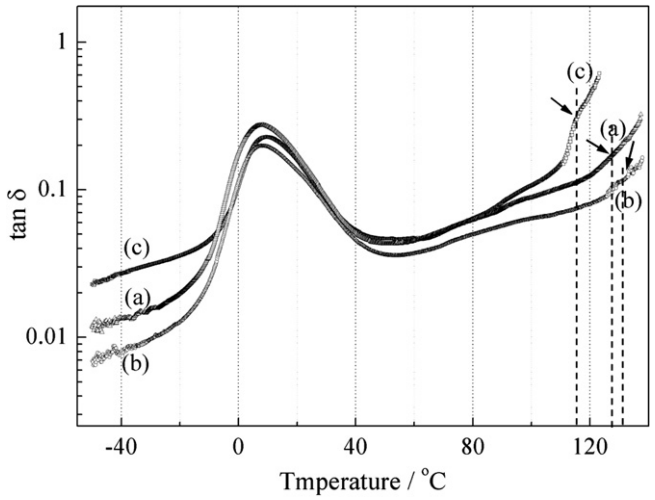

Fig. 12. Temperature dependence of tanδ of (a) PHBV18HHx11, (b) PHBV7HHx11 and (c) PHBHHx12, which are all isothermally crystallized at 90 °C. The arrow indicates T_{m1} of each sample.

4. Conclusion

PHBVHHx showed higher crystallization rate and higher degree of crystallinity than PHBHHx12 did. The terpolyesters exhibited different multiple melting behaviors compared with PHBHHx. The crystal structure of PHBVHHx was more compact than PHBHHx, indicating the stronger hydrogen bonding between chain stems in the crystal lattice of the former. This explains the higher crystallization rate and higher degree of crystallinity of PHBVHHx compared with PHBHHx. During heating, PHBVHHx showed a partial melting-lamellar thickening–remelting process, while PHBHHx demonstrated a melting-quickly formation of new lamellae-remelting process. All the above results demonstrate that the simultaneous introduction of 3-hydroxyvalerate (3HV) and 3-hydroxyhexanoate (3HHx) monomers enhanced the degree of crystallinity of the terpolyester and improved the tendency of lamellar reorganization during melting and tensile drawing, resulting in improved mechanical properties. Terpolymerization may point to a new way to improve the properties of PHA. Futhermore, our results demonstrate that there is a close link between the lamellar reorganization during hearing and tensile drawing.

Acknowledgements

This work was partially supported by the National Natural Science Foundation of China (Grant Nos. 20504019, 50673050, and 20974060). Li Ka-Shing Foundation and National High Tech 863 Grant (Project No. 2006AA02Z242 and 2006AA020104), as well as the State Basic Science Foundation 973 (2007CB707804) and Guangdong Provincial Grant for collaboration among industry, university and research organization awarded to GQC were also contributed to this study.

References

[1] Chen GQ. Chem Soc Rev 2009;38:2434–46.
[2] Lee SY. Biotechnol Bioeng 1996;49:1–14.
[3] Steinbüchel A, Füchtenbusch B. Trens Biotechnol 1998;16:419–27.

[4] Scandola M, Ceccorulli G, Pizaaoli M. Macromol Chem Rapid Commun 1989;10:47–50.
[5] de Koning GJM. ACS Symp Ser 1994;575:188–201.
[6] Madden LA, Anderson AJ. Polymer 2000;41:3499–505.
[7] Asrar J, Valentin HE, Berger PA, Tran M, Padgette SR, Garbow JR. Biomacromolecules 2002;3:1006–12.
[8] Zhao W, Chen GQ. Process Biochem 2007;42:1342–7.
[9] Zhang HF, Ma L, Wang ZH, Chen GQ. Biotechnol Bioeng 2009;104:582–9.
[10] Gunaratne LMWK, Shanks RA, Amarasinghe G. Therm Acta 2004;423:127–35.
[11] Gunaratne LMWK, Shanks RA. Therm Acta 2005;430:183–90.
[12] Gunaratne LMWK, Shanks RA. Eur Polym J 2005;41:2980–8.
[13] Owen AJ, Heinzel J, Škrbić Ž, Divjaković V. Polymer 1992;33:1563–7.
[14] Chen SS, Liu Q, Wang HH, Chen GQ, Inoue Y. Polymer 2009;50:4378–88.
[15] Doi Y, Kitamura S, Abe H. Macromolecules 1995;28:4222–8.
[16] Abe H, Doi Y, Aoki H, Akehata T. Macromolecules 1998;31:1791–7.
[17] Feng L, Watanabe T, Wang Y, Kichise T, Fukuchi T, Chen GQ. Biomacromolecules 2002;3:1071–7.
[18] Xu J, Guo BH, Yang R, Wu Q, Chen GQ. Polymer 2002;43:6893–9.
[19] Wu Q, Tian G, Sun SQ, Noda I, Chen GQ. J Appl Polym Sci 2001;82:934–40.
[20] Hu Y, Zhang J, Sato H, Noda I, Ozaki Y. Polymer 2007;48:4777–85.
[21] Sato H, Nakamura M, Padermshoke A, Yamaguchi H, Terauchi H, Ekgasit S. Macromolecules 2004;37:3763–9.
[22] Sato H, Padermshoke A, Nakamura M, Murakami R, Hirose F, Senda K. Macromol Symposia 2005;220:123–38.
[23] Sato H, Murakami R, Padermshoke A, Hirose F, Senda K, Noda I. Macromolecules 2004;37:7203–13.
[24] Padermshoke A, Sato H, Katsumoto Y, Ekgasit S, Noda I, Ozaki Y. Vib Spectrosc 2004;36:241–9.
[25] Chen C, Cheung MK, Yu PHF. Polym Int 2005;54:1055–64.
[26] Chen GQ, Zhang G, Park SJ, Lee SY. Appl Microbiol Biotechnol 2001;57:50–5.
[27] Fukui T, Abe H, Doi Y. Biomacromolecules 2002;3:618–24.
[28] Lu XY, Zhang WJ, Wu Q, Chen GQ. FEMS Microbiol Lett 2005;243:149–55.
[29] Wang HH, Li XT, Chen GQ. Process Biochem 2009;44:106–11.
[30] Xu J, Guo B-H, Zhang Z-M, Zhou J-J, Jaing Y, Yan S, et al. Macromolecules 2004;37:4118–23.
[31] Wang X, Zhou J, Li L. Eur Polym J 2007;43:3163–70.
[32] Morra BS, Stein RS. J Polym Sci Polym Phys Ed 1982;20:2243–59.
[33] Krache R, Benavente R, López-Majada JM, Pereña JM, Cerrada L, Pérez E. Macromolecules 2007;40:6871–8.
[34] Yokouchi M, Chatani Y, Tadokoro H, Teranishi K, Tani H. Polymer 1973;14:267–72.
[35] Brückner S, Meille SV, Malpezzi L, Cesaro A, Navarini L, Tombolini R. Macromolecules 1988;21:967–72.
[36] Orts WJ, Marchessault RH, Bluhm TL, Hamer GK. Macromolecules 1990;23:5368–70.
[37] Iwata T, Fujita M, Aoyagi Y, Doi Y, Fujisawa T. Biomacromolecules 2005;6:1803–9.
[38] Gazzano M, Tomasi G, Scandola M. Macomol Chem Phys 1997;198:71–80.
[39] Sato H, Dybal J, Murakami R, Noda I, Ozaki Y. J Mol Struct 2005;744–747:35–46.
[40] Sato H, Mori K, Murakami R, Ando Y, Takahashi I, Zhang JM, et al. Macromolecules 2006;39:1525–31.
[41] Doi Y, Kitamura S, Abe H. Macromolecules 1995;28:4822–8.
[42] Saito M, Inoue Y. Macromolecules 2001;34:8953–60.